Earth and Planetary Science Letters, 98 (1990) 154–165
Elsevier Science Publishers B.V., Amsterdam – Printed in The Netherlands

[CH]

Some isostatic and thermal consequences of the vertical strain geometry in convergent orogens

Michael Sandiford [1] and Roger Powell [2]

[1] *Department of Geology and Geophysics, University of Adelaide, GPO Box 498, Adelaide, S.A. 5001 (Australia)*
[2] *Department of Geology, University of Melbourne, Parkville, Vic. 3502 (Australia)*

Received July 11, 1989; revised version accepted February 12, 1990

The thermal and isostatic consequences of continental deformation, particularly surface elevation, horizontal buoyancy forces and metamorphism in the crust, depend to a considerable extent on the way in which strain is distributed between the crust and the mantle lithosphere [1]. Since these vertical strains may be strongly "decoupled" by processes such as convective thinning or detachment of the lower thermal boundary layer [2], with the extent of this "decoupling" varying in space and time in an orogen [3], it is useful to parameterise the vertical strain on the scale of the crust, f_c, and lithosphere, f_l, respectively. We illustrate this parameterisation by considering the thermal and isostatic consequences of a number of f_c–f_l paths which may develop during the convergent deformation of a thermally-stabilised lithosphere. Three qualitatively distinct f_c–f_l paths in orogens are distinguished on the extent of "decoupling" between vertical strains in the crust and mantle lithosphere. *Type 1 paths* involve no decoupling, so the vertical strain in the lithosphere is homogeneous. For a given f_c, Type 1 paths result in relatively low surface elevation and low-intermediate metamorphic temperatures appropriate for the development of glaucophane-schist and Barrovian metamorphic assemblages. *Type 2 paths* allow decoupling due to processes such as convective thinning of the mantle lithosphere on the orogenic timescale but only after considerable initial lithospheric thickening. Type 2 paths lead to relatively high surface elevations, for a given f_c, and intermediate to high metamorphic temperatures only after the mantle lithosphere is thinned. The increase in potential energy associated with mantle lithospheric thinning (resulting in an increase in buoyancy forces by as much as 10^{13} Nm^{-1}) will quickly terminate convergent deformation, with the result that metamorphic heating will postdate the thickening deformation, and may induce extensional collapse of the orogen. *Type 3 paths* involve efficient mantle lithosphere thinning as the crust thickens with a consequence being, particularly, the possibility of relatively high metamorphic temperatures during active crustal thickening. For a given driving force, convergent deformation along a Type 3 path will be terminated at relatively small f_c providing an appropriate setting for the development of high T–low P metamorphic assemblages.

1. Introduction

The physical properties (density, strength, heat production etc.) of the lithosphere vary dramatically with depth due to changing temperature and composition, and therefore it is possible that lithospheric deformation is markedly heterogeneous in the vertical dimension. In particular, the crust–mantle boundary represents an important compositionally-defined rheological boundary across which strains may be partitioned. Any description of lithospheric deformation should therefore allow the possibility that crustal strain is "decoupled" from the strain in the subcrustal mantle lithosphere [1–5]. Moreover, the thermal structure and mechanical properties of orogens evolve primarily as a consequence of relative changes in the thickness of the crust and the mantle lithosphere (that is, as a consequence of vertical strains). Although the vertical strain geometry is likely to be more complex, we propose to describe lithospheric deformations in terms of just two parameters: a crustal thickening factor, f_c, defined as the ratio of the thickness of deformed crust to initial crust; and a lithospheric thickening factor, f_l, defined as the ratio of the thickness of deformed lithosphere to initial lithosphere (note that we use *lithosphere* to include both the crust and upper non-convective mantle) [1,6,7]. Using the f_c–f_l parameterisation, the deformation in any part of an orogen can be described in terms of an f_c–f_l path showing how crust and lithosphere thickness have changed

0012-821X/90/$03.50 © 1990 – Elsevier Science Publishers B.V.

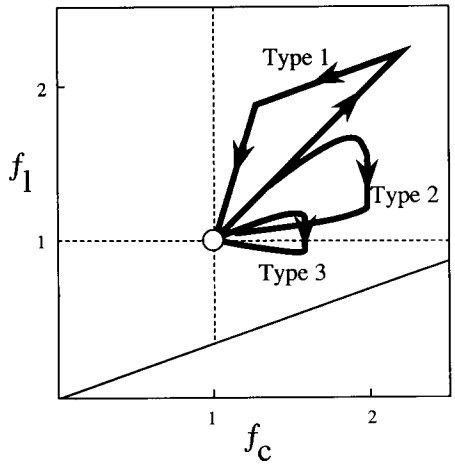

Fig. 1. Deformation paths on the f_c–f_l plane. Type 1, 2 and 3 paths are discussed in the text.

with time; such paths reflect not only the vertical strain on the crust and lithosphere scale at any time during deformation, but also the effect of all other processes which may change crust and lithosphere thickness as a consequence of the strain, for example crustal erosion and convective thinning of the mantle lithosphere.

f_c–f_l paths may be portrayed on the f_c–f_l plane, e.g. Fig. 1. We will normally draw the f_c–f_l plane with an origin at $f_c = 1$ and $f_l = 1$ corresponding to "equilibrium" lithosphere, the (hypothetical) state that the crust and lithosphere tends to with time. This lithosphere will be taken as the material input into the orogen. Also, as a consequence, f_c–f_l paths will tend to be closed paths, starting at the origin ($f_c = f_l = 1$) and finishing there, eventually. Note that, on the f_c–f_l plane, there is an inaccessible region at low f_l and high f_c, the boundary of which is when the lithosphere consists entirely of crust. Defining ψ as the initial ratio of crust to lithosphere thickness, z_c/z_l, where z_c is the initial crust thickness and z_l is the initial lithosphere thickness, this boundary is given by $f_l = f_c/\psi$. Considering types of paths on the f_c–f_l plane, homogeneous strain paths, with crust and lithosphere changing thickness in the same proportion, have unit slopes, for example the first segment of the Type 1 path on Fig. 1. A path involving a change in lithosphere thickness without a change in crust thickness is a vertical line; however a path involving a change of crust thickness without a change in *mantle* lithosphere thickness, does involve a change of lithosphere thickness; such paths are parallel to the boundary of the inaccessible region, having a slope of $1/\psi$, for example the second, erosion-driven segment of the Type 1 path on Fig. 1.

The f_c–f_l plane not only allows the portrayal of the f_c–f_l paths, for example, for orogenic belts or parts thereof, but also the plane may be contoured for some important isostatic and thermal consequences of deformation, for example the isostatically supported change in elevation induced by the deformation, Figs. 2–5. Once deformation starts,

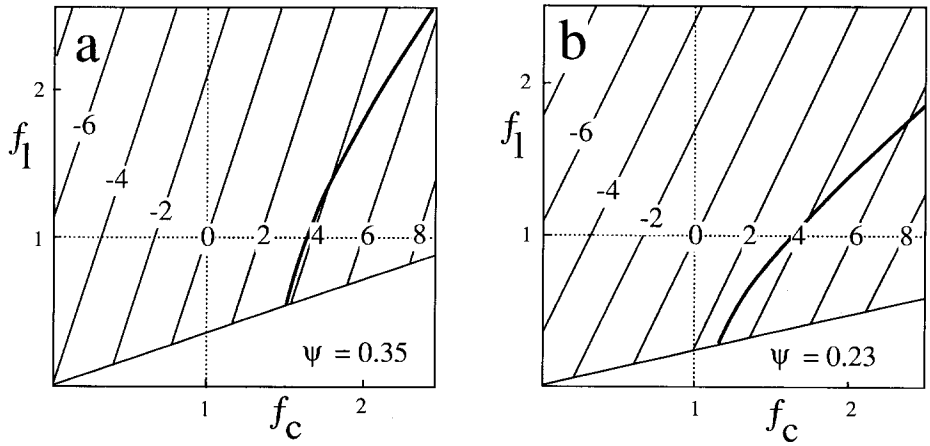

Fig. 2. The f_c–f_l plane contoured for the isostatically supported change in surface elevation. The contours are for h calculated using eqn. (1) (with $z_c = 35$ km); the contour interval is 2 km. $\alpha T_l = 0.0375$ (e.g., for $\alpha = 3\times10^{-5}\mathrm{K}^{-1}$ and $T_l = 1250\,^\circ$C); $\delta = \rho_c/\rho_l = 0.833$ (e.g. for $\rho_c = 2750$ kg m^{-3} and $\rho_l = 3300$ kg m^{-3}). A reference force of 5×10^{12} Nm^{-1} is shown as a bold line, see Fig. 3. (a) is for $\psi = z_c/z_l = 0.35$; (b) is for $\psi = 0.23$.

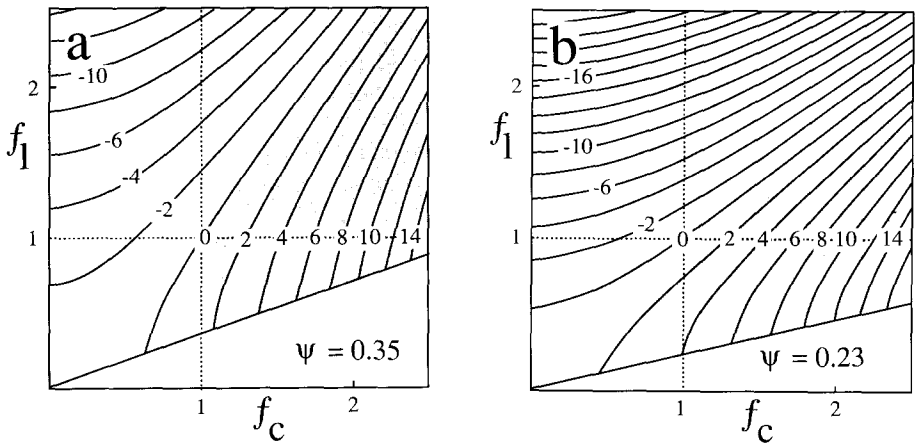

Fig. 3. The f_c–f_1 plane contoured for the induced horizontal buoyancy force, F_b, between deformed and undeformed lithosphere assuming local isostatic compensation using eqn. (2) (with $z_c = 35$ km and $\rho_c = 2750$ kg m^{-3}); the contour interval is 2×10^{12} Nm^{-1}. In the text, $F = 5\times10^{12}$ Nm^{-1} (equivalent to the 1.5 contour) is taken, somewhat arbitrarily as the tectonic driving force in lithospheric deformation. (a) is for $\psi = z_c/z_l = 0.35$; (b) is for $\psi = 0.23$.

and an f_c–f_1 path initiated, there are isostatic and thermal consequences reflected in the crossing of contours, and, as a result, the path will be affected. The overall f_c–f_1 path is controlled by the interaction between the driving force for the deformation and its consequences. In order to model the evolution of an orogen it is necessary to solve the appropriate three-dimensional governing equations subject to a sufficient set of boundary conditions and, for computational feasibility, appropriate approximations [e.g. 8–9]. This is not our intention here; rather we show how the simple one-dimensional f_c–f_1 parameterisation allows many important isostatic and thermal consequences of an orogenic deformation to be easily evaluated. By examining the isostatic and thermal

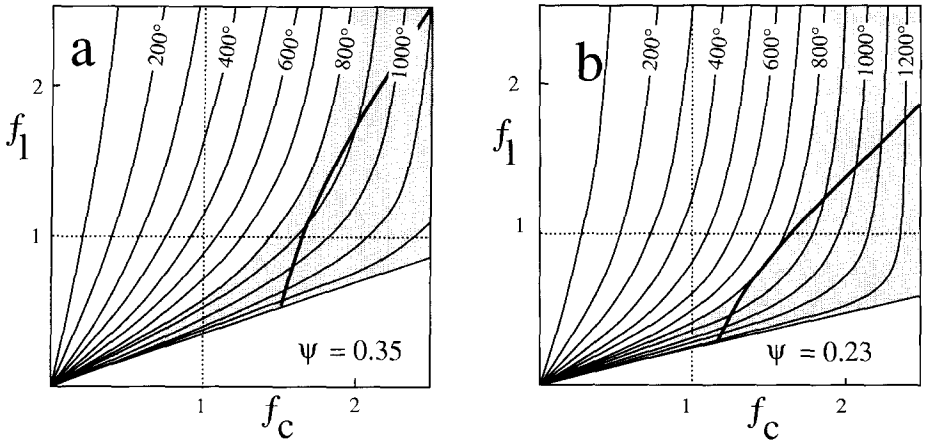

Fig. 4. The f_c–f_1 plane contoured for potential Moho temperature (i.e., $T_{c,p=1}$) using eqn. (3); the contour interval is 100 °C. Parameters as in Fig. 2. A conductivity of 3 W m^{-1} K^{-1} and a uniform distribution of heat sources in the crust is assumed to give an initial surface heat flow of 55 mW m^{-2}. A reference force of 5×10^{12} Nm^{-1} is shown as a bold line, see Fig. 3. (a) is for $\psi = z_c/z_l = 0.35$; (b) is for $\psi = 0.23$. Compare with Fig. 11 constructed for half crustal depth ($p = 1/2$). The stippled region corresponds to deformation geometries which have the potential for lower crustal heating sufficient to generate significant volumes of melt, i.e., $T_{c,p=1} > 800$ °C (see Fig. 4a). For these geometries the potential thermal structure at shallower crustal levels may be significantly modified by magmatic advection of heat.

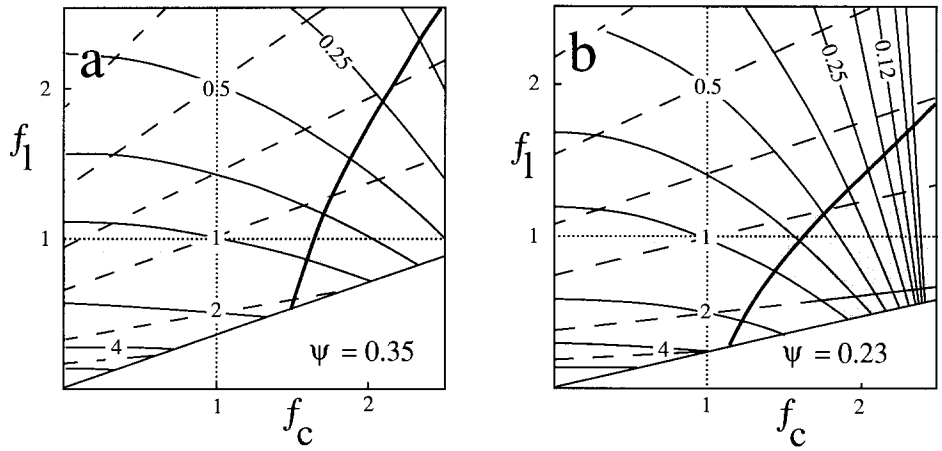

Fig. 5. The f_c–f_l plane contoured for changes in r_0 (dashed lines) and r_p (solid lines), see text. Parameters as in Fig. 2. A reference force of 5×10^{12} Nm^{-1} is shown as a bold line, see Fig. 3. (a) is for $\psi = z_c/z_l = 0.35$; (b) is for $\psi = 0.23$.

consequences of hypothetical convergent deformations in a thermally-stabilised lithosphere, we illustrate how the use of the f_c–f_l parameterisation may allow discrimination of a number of different lithospheric-scale vertical strain histories in modern and ancient orogenic belts. In particular we hope to emphasize, through the use of the f_c–f_l parameterisation, the importance of explicitly incorporating a description of mantle lithospheric deformation in any attempt to understand the thermal and mechanical evolution of orogenic belts.

2. Isostatic consequences

Assuming isostatic compensation, the change in elevation and the potential energy of an orogen are a function of the vertical strain geometry, given by f_c and f_l, and of the density structure of the lithosphere, which is related to the relative thickness of the crust and mantle and, to a lesser extent, the thermal structure of the lithosphere. Provided isostatic compensation is maintained, the elevation and potential energy of an orogen are independent of the deformation path, and thus the isostatic consequences of any deformation can be illustrated on the f_c–f_l plane (Figs. 2a, b, 3a, b).

The change in elevation, h, is approximately (all the equations are derived in the Appendix):

$$\frac{h}{z_c} = (1-\delta)(f_c - 1) - \frac{\alpha T_l}{2\psi}(f_l - 1) \qquad (1)$$

where $\delta = \rho_c/\rho_l$, with ρ_c and ρ_l the densities at T_l of crust and mantle respectively; $\psi = z_c/z_l$, with z_c and z_l the initial thickness of the crust and mantle respectively; α is the coefficient of thermal expansion of crust and mantle, and T_l is the temperature at the base of the lithosphere (we assume also that the surface temperature is 0 so that T_l is also the temperature difference across the lithosphere). We assume a simple density structure ($\rho_c \sim 2750$ kg m^{-3}, $\rho_l \sim 3300$ kg m^{-3}) with the thickness of "typical" continental crust, z_c, taken to be 35 km. As the initial thickness of the lithosphere, z_l, is poorly defined, we have evaluated the effect of deformations for two different initial lithospheric thicknesses: 100 km and 150 km, corresponding to $\psi = 0.35$ and 0.23, respectively. We treat the lithosphere as thermally stabilised, extending to the base of the lower thermal boundary layer, with $T_l = 1250\,^\circ$C [10].

Figures 2a and b show that crustal thickening and mantle lithospheric thinning favour uplift, while crustal thinning and mantle lithospheric thickening favour subsidence. The slope of the elevation contours are directly proportional to ψ; with increasing ψ, they swing to steeper orientations in f_c–f_l space because there is proportionately less lithospheric upper mantle contributing to the elevation. For $\psi = 0.18$, homogeneous deformations (that is, $f_c = f_l$) produce no change in surface elevation for the density structure assumed here.

The change in potential energy resulting from deformation can be represented as the horizontal buoyancy force per unit length of orogen, F_b, in

Nm^{-1}, arising from lateral differences in the vertical stress contributed by differences in density distribution with depth (particularly at the surface and at the Moho) between the deformed and adjacent undeformed lithosphere (see the Appendix):

$$\frac{F_b}{\rho_1 z_c^2} = \delta\frac{1-\delta}{2}\left(f_c^2 - 1\right) - \frac{\alpha T_1}{6\psi^2}\left[f_1^2 - 1 - 3(1-\delta)(f_c f_1 - 1)\right] - \frac{\alpha^2 T_1^2}{8\psi^2}\left(f_1^2 - 1\right) \quad (2)$$

Figures 3a and b show that crustal thickening and mantle lithosphere thinning result in extensional forces within the orogen, while crustal thinning and mantle lithosphere thickening result in compression (neglecting any forces applied across the boundary of the orogen). Buoyancy force contours swing to shallower orientations with decreasing ψ. For $\psi = 0.29$ (and the density structure modelled here) homogeneous thickening deformations produce no change in the potential energy of the lithosphere since the excess potential of thickened buoyant crust is offset by a corresponding deficit provided by the thickened dense mantle lithosphere.

f_c–f_1 plots contoured for F_b must be understood in terms of the externally applied forces across the orogen and the strength of the lithosphere. In the absence of an externally applied tectonic driving force, the buoyancy force resulting from variations in crustal and lithospheric thickness, for example, between our deformed lithosphere and the adjacent normal lithosphere, may cause deformation, tensional if $F_b > 0$, compressional if $F_b < 0$, if the strength of the lithosphere is overcome. On the f_c–f_1 plane the strength of the lithosphere can be represented by a band which encompasses the range of crustal and lithospheric thicknesses (f_c and f_1) which are in potential energy balance within the limits of the strength of the lithosphere. The band which in the static case passes through the origin ($f_c = f_1 = 1$) is asymmetric about the origin because lithosphere is stronger in compression than tension and its width depends on the geotherm, among other things, because of the strong temperature dependence of lithospheric rheologies (moreover, since the geotherm changes as a consequence of the deformation the strength of the lithosphere and hence the width of the band will show temporal variations through the orogenic process). With externally applied forces, the band will be shifted so that it is located about the F_b contour corresponding to the driving force (F_d) applied across the boundary of the deformed zone. For a compressional driving force (F_{dc}), the band occurs in the $F_b > 0$ field with the lower boundary corresponding to the buoyancy force equivalent to the applied force minus the strength of the lithosphere. This lower boundary can be thought of as the limiting effective driving force (F_{edc}) for convergent deformation because the lithosphere cannot be deformed to a larger f_c across this boundary. Thus, deformation paths involving increasing F_b (for example, homogeneous deformation with $\psi > 0.29$, Fig. 3a), must be self-limiting, with the limit applying when F_b is of the same order as this limiting effective driving force. This contrasts with deformation paths involving decreasing F_b (for example, homogeneous deformation with $\psi < 0.29$, Fig. 3b) and highlights the importance of the ratio ψ in determining the behaviour of convergent orogens.

3. Thermal consequences

Analytic solutions to the thermal evolution of lithosphere deformed at finite rates cannot generally be obtained. Moreover, because of the low thermal conductivity of rocks the thermal consequences of deformation are dependent not only on the value of f_c and f_1 but also on the deformation path and, particularly, the strain rates. However, it is useful to illustrate on the f_c–f_1 plane the limiting temperatures attainable due to the thermal equilibration of the deformed lithosphere since they provide a natural bound on the range of temperatures achievable during metamorphism (in the absence of magmatic redistribution of heat!). We define the *potential temperature* as the temperature that would eventually result at any specified level in the lithosphere as a consequence of the conductive equilibration of the deformed lithosphere, assuming some initial distribution of heat source; for very slow strain rates a deforming orogen would achieve and maintain this *potential* thermal state. The potential temperature, T_c, for

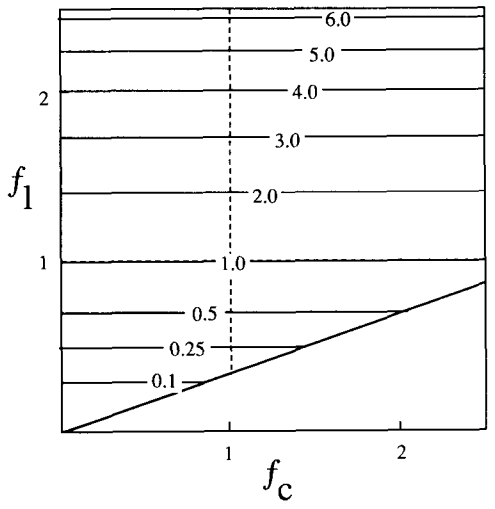

Fig. 6. The $f_c - f_1$ plane contoured for $\tau'(\tau' = \tau_1/\tau_0)$, where τ_0 is the thermal time constant for the initial lithosphere and τ_1 is the thermal time constant for the deformed lithosphere.

any material point at depth $p = z/z_c$ within the *initial* crust, with a homogeneously distributed volumetric heat production in the crust giving an initial temperature at the base of crust of T_c^0, is given by (assuming deformation on the crustal scale is homogeneous):

$$\frac{T_c}{T_c^0} = \frac{p}{\gamma}\left[\frac{f_c}{f_1}\psi - f_c^2\left(p - 2 + \psi\frac{f_c}{f_1}\right)\left(\frac{\gamma - \psi}{1 - \psi}\right)\right] \quad (3)$$

where $\gamma = T_c^0/T_1$. During the deformation history, the depth of the material point for which the potential temperature is calculated is just pf_c, as deformation on the crustal scale is assumed to be homogeneous.

The potential thermal structure will only be approached if the deformed lithosphere is maintained for a time interval of the order of the thermal time constant, τ_1, of the lithosphere. Since the thermal time constant is proportional to the square of the length scale of the perturbation, thinned lithosphere is much more likely to attain its potential thermal structure than thickened lithosphere (Fig. 6). Given that orogens have finite lifetimes of the order of 10–100 Ma (that is, equivalent to the thermal time constant of lithosphere 20–60 km thick) the isotherms in the lower third of Figs. 4a and b are likely to be realistic estimates of the thermal structure developed as a consequence of natural deformations. In contrast, an increasing disparity between the potential thermal structure and the actual thermal structure attained in natural deformations is to be expected with increasing f_1.

The potential thermal structure may also be more closely approached if, following the end of deformation, f_c and f_1 do not change further. However, this is unlikely in the case of the thermally stabilised lithosphere considered here. We assume that the initial lithospheric structure represents a thermal equilibrium dictated by balancing the heat supplied to the base of the lithosphere (from convective motion in the subjacent asthenosphere) with heat loss through the mantle part of the lithosphere, q_m. Lithospheric deformations will, in general, produce significant departures from this initial equilibrium, and consequently there will be a tendency for further change in lithospheric thickness in order to re-establish the thermal equilibrium (we assume that the heat supplied to the lithosphere is invariant over the lifespan of an individual orogen). The classic example of this behaviour is provided by the conductive thickening of the mantle lithosphere associated with thermal sag following homogeneous lithospheric extension (Fig. 7) [11], and which provides strong support for the notion that the lower part of the continental lithosphere is indeed thermally stabilised. Homogeneous thickening of a thermally stabilised lithosphere in a convergent orogen will have the opposite effect to extension; it will in-

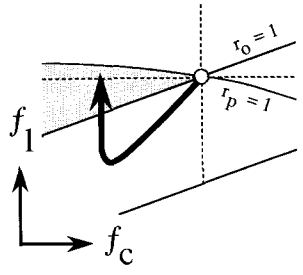

Fig. 7. Evolution of a stretched basin on the $f_c - f_1$ plane. Homogeneous stretching produces rift phase subsidence ($f_c = f_1 < 1$), followed by sag phase subsidence associated with thickening of the mantle lithosphere due to conductive heat loss in search or $r = 1$. Sag phase subsidence outlasts active rifting because the thermal conductivity of the lithosphere is such that thickening due to conductive heat loss (i.e., the rate at which the $r = 1$ condition is attained) is much slower than typical extensional strain rates. In the path shown here the effects of sedimentation have been ignored. With sedimentation the $f_c - f_1$ path will form a closed clockwise loop terminating at the origin.

duce the potential for lithospheric thinning in order to balance heat supply. We characterise this tendency for the lithosphere thickness to change by r, the proportional change to lithosphere thickness needed to re-establish an equilibrium heat flux for a given f_c. If the lithosphere thickness during or at the end of deformation is $f_1 z_1$, then the equilibrium thickness is $r f_1 z_1$. The equilibrium condition towards which the lithosphere will evolve is the condition $r = 1$. Deformations which significantly decrease mantle lithosphere thickness ($r > 1$) induce the potential for further mantle lithospheric thickening, while deformations which significantly thicken the mantle lithosphere ($r < 1$) induce the potential for further mantle lithosphere ($r < 1$) induce the potential for further mantle lithospheric thinning (Figs. 5a and b). Since analytic solutions to the thermal evolution of the lithosphere deformed at finite geological rates are not generally available, we provide two limiting solutions for r: the first, r_0, appropriate to a thermal structure in which no heating or cooling has taken place during the deformation path:

$$r_0 = \frac{1 + \psi(f_c - 1)}{f_1} \tag{4}$$

and the second, r_p, appropriate to the potential thermal structure of the orogen:

$$r_p = \frac{1 - \psi - f_c^2(\gamma - \psi)}{f_1(1 - \gamma)} \tag{5}$$

These two cases are appropriate to an instantaneous deformation path and an infinitely slow deformation path, respectively. For natural deformations the instantaneous value of $r = 1$ will track from $r_0 = 1$ to $r_p = 1$ during the lifetime of the orogen.

4. Vertical strain history of convergent orogens

In order to model the thermal and mechanical evolution of a thermally-stabilised continental lithosphere in a convergent orogen it is important to specify the rate at which deformed lithosphere changes its thickness to balance heat supply (that is, in order to attain the $r = 1$ condition). If the condition $r = 1$ is attained only by conductive heat transfer then the rate of change is likely to be slow compared to orogenic strain rates (for example, the time scale of the sag-phase episodes in stretched basins is typically much longer than the preceding rift-phase episodes [11]). However if attainment of the $r = 1$ condition is facilitated by convective heat transfer processes, for example by convective thinning of a thickened lower thermal boundary layer at the base of the lithosphere [2], it may occur at a rate which is comparable to or faster than the orogenic strain rate [3]. Indeed the numerical experiments of Houseman et al. [2] show that convective thinning of thickened thermal boundary layer at the base of the lithosphere may be very fast compared to orogenic strain rates; the rates are however likely to be strongly dependent on the convective vigour of the asthenosphere and are not well constrained. To date there are few observations pertinent to the behaviour of the mantle lithosphere beneath continental orogens, and we therefore consider three *hypothetical* limiting paths which encompass the range of likely possibilities (Fig. 1). Using the f_c–f_1 parameterisation we show that qualitatively different isostatic and thermal responses may be expected for these three paths. These different responses are reflected primarily in the elevation of the orogen and also the way in which the incremental vertical strain history evolves with time and the thermal state of the orogen. Consequently, observations bearing on the elevation and the thermal state of an orogen potentially allow the means of evaluating the behaviour of the lithosphere in both modern and ancient orogenic belts and may therefore be used to reconstruct the f_c–f_1 path of orogens, or parts thereof. The three hypothetical paths which we consider explicitly are:

Type 1 paths involving homogeneous deformation with $f_c = f_1$ (i.e., crustal and mantle strains are coupled). In this case the mantle lithosphere is not able to adjust its thickness to balance heat supply with heat loss on the time scale appropriate to the construction and subsequent denudation of the orogen. The isostatic consequences of Type 1 paths are critically dependent on the value of ψ.

Type 2 paths allow decoupling of the crust and mantle lithospheric deformation but only after considerable initial homogeneous thickening [e.g. 2]. Explicitly, Type 2 paths involve initially homogeneous deformation paths with $f_c = f_1$ which then depart into $f_c > f_1$ in search of $r = 1$. The consequences of Type 2 paths are dependent primarily

on the timing of onset, and rate, of lithospheric thinning with respect to shortening strains.

Type 3 paths in which the rate of adjustment of mantle lithosphere thickness to balance heat supply is assumed to be fast compared to orogenic strain rates, such that the instantaneous value of r is always 1.

For Type 1 paths a limit to convergent deformation will necessarily prevail only if the deformation induces an increase in potential energy, with the limit applying when the horizontal buoyancy force, F_b, is equal but opposite to the limiting effective driving force (F_{edc}) for convergent deformation. Absolute driving forces for plate tectonics are of the order of $10^{13}\mathrm{Nm}^{-1}$, and here we arbitrarily consider the limiting effective driving force, F_{edc}, of 5×10^{12} Nm^{-1}. Homogeneous deformation of a lithosphere with $\psi > 0.29$ will produce an increase in the potential energy of the orogen (relative to the initial lithosphere), and thus the total lithospheric thickening must be self-limiting; Fig. 2a shows that for $\psi = 0.35$ and $F_{edc} = 5 \times 10^{12}\mathrm{Nm}^{-1}$ the limit will occur at values of $f_c \sim 2.0$ when a surface elevation of some 3–4 km has been attained. If the limit is attained in any part of the orogen, further convergent deformation must be distributed elsewhere, allowing the possibility for the formation of a broad orogenic plateau. If the driving forces wane, or if constraints along the lateral boundaries of the orogen are relieved to the extent that F_b exceeds the limiting effective strength for extensional deformation (F_{edt}) then the orogen may collapse by extension, otherwise it will denude by erosion, each scenario producing a characteristic path in f_c–f_l space (Fig. 8). Since the strength of rocks in tension is less than in compression, the complete reduction of driving forces will necessarily be sufficient to initiate extension provided $F_{edt} - F_{dc} < F_{edc}$ (Fig. 8b). However extension could only continue while the horizontal buoyancy forces exceed the tensional strength of the lithosphere ($F_b > F_{edt}$) a condition which is likely to attain only while considerable topography remains. Further denudation would be restricted to erosion first towards low surface elevation, and then slowly back to $f_c = 1$ and $f_l = 1$ as thermal relaxation towards $r = 1$ takes place (Fig. 8b). Type 1 paths with $\psi < 0.29$ will not necessarily be self limiting since the buoyancy forces resulting from progressive deformation enhance the driving forces for convergence and potentially allow the possibility of self-localising deformation. One important consequence may be the development of very thick crust ($f_c > 2.0$) even for relatively small driving forces (a minimum necessary driving force is provided by the strength of the lithosphere). Despite the extreme crustal thicknesses achievable under such circumstances topography need not be extreme (~ 3 km for $f_c = 2$ with $\psi = 0.23$, Fig. 2b; 0 km for all f_c with $\psi = 0.18$). A reduction in the convergent driving force may have little effect as the thickened lithosphere develops its own "pull" in an analogous fashion to subducting oceanic lithosphere (for old oceanic lithosphere $\psi \sim 0.06$). Denudation of the resulting surface topography must occur by erosion. It is interesting to note that while we know of no modern convergent orogens in which f_c is currently greater than ~ 2, the very high-pressure metamorphic rocks of the Dora

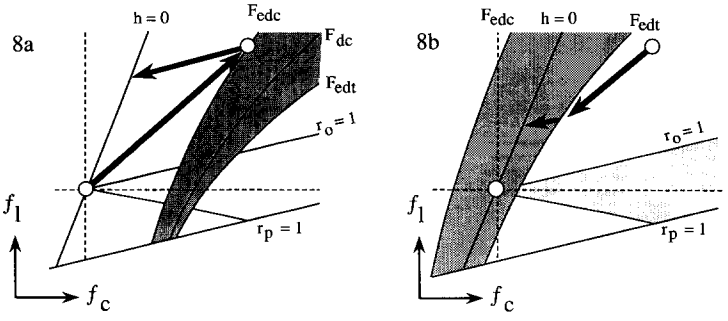

Fig. 8. Evolution of a Type 1 path with $\psi \gg 0.29$ on the f_c–f_l plane. Figure 8a shows the deformation path for an orogen terminated by erosion which reduces all topography to that of the initial lithosphere (that is the $h = 0$ condition). Figure 8b shows the evolution of an orogen where extension follows the waning of the driving force for convergence (see text for discussion). The effective strength envelope represents the difference between the driving force, F_{dc}, and the force required to deform the lithosphere at a significant rate (F_{edc} for compression, F_{edt} for tension).

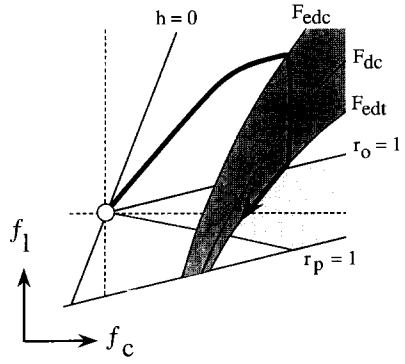

Fig. 9. Evolution of a Type 2 path on the f_c–f_l plane, see text for discussion.

Maira in the western Alps [12] testify to the existence of an extraordinarily thick crust ($f_c \sim 3.0$) at some earlier stage in Alpine history, which may reflect the homogeneous deformation ($f_c = f_l$) of a low ψ-lithosphere.

Somewhat different histories are likely for Type 2 paths where, at some stage during or after homogeneous thickening, the mantle will begin to evolve towards the $r = 1$ condition (Fig. 9). Deformation paths will deviate towards the $f_c > f_l$ field with attendant increases in the surface elevation and potential energy. The increase in potential energy, which may amount to as much as 10^{13} Nm^{-1} equivalent, will eventually result in the development of horizontal buoyancy forces which are equal, but opposed, to F_{edc}. When this occurs convergent deformation must then be partitioned elsewhere. With continued mantle lithospheric thinning in search of the equilibrium condition $r = 1$, a significant increase in both the elevation and the potential energy of the orogen result with the possibility of $F_b > F_{dc}$ (Fig. 9). If F_b exceeds the driving force by an amount greater than the effective tensional strength of the lithosphere, that is $F_b > F_{edt}$, then the consequences may be dramatic, with the possibility of extensional collapse, particularly if the driving force wanes (Fig. 9). However, it is important to realise that Type 2 paths may induce collapse without a reduction in driving forces. For a constant driving force, F_{dc}, collapse will be buffered along f_c–f_l paths dictated by the effective strength envelope (Fig. 9) of the lithosphere with deformation terminating with the attainment of the condition $r = 1$. Return of the deformed lithosphere to $f_c = 1$ and $f_l = 1$ will take place by erosion with maintenance of $r = 1$.

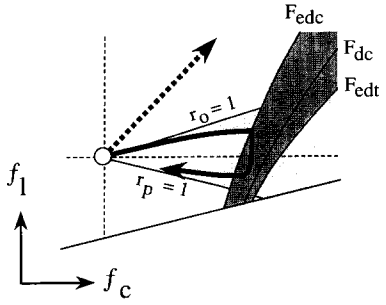

Fig. 10. Evolution of a Type 3 path on the f_c–f_l plane, see text for discussion.

Type 3 paths evolving always with $r = 1$ (Fig. 10) will, independently of the value of ψ, produce sufficient increases in potential energy to limit the deformation with relatively small finite crustal thickening strains ($f_c \sim 1.6$ for $F_{ed} = 5 \times 10^{12}$ Nm^{-1}). Subsequent partitioning of convergent deformation elsewhere should build broad plateaus with relatively high elevations for the crustal thickness. Since the $r = 1$ contour is approximately at right angles to the F_b contours Type 3 paths evolve along a condition of maximum potential energy and therefore collapse can only be initiated by the waning of driving forces in which case the deformation will map out a clockwise loop in f_c–f_l space (Fig. 10).

5. Thermal evolution of convergent orogens

The three f_c–f_l paths considered here have important implications for the thermal evolution of the lithosphere. In particular, the heat flow through the mantle part of the lithosphere, q_m, is sensitive to the vertical strain geometry, and we conclude by briefly considering the thermal consequences of the three types of behaviour described in the preceding section (a detailed discussion of the thermal consequences of Type 3 paths is presented elsewhere [13]).

Because of the long times required for thermal equilibration of homogeneously thickened lithosphere (Fig. 6), Type 1 paths are unlikely to lead to the realization of the potential thermal structure (Figs. 4a, b) during active thickening, and heating should continue well beyond such thickening. For a given f_c the total potential crustal heating is relatively limited since q_m decreases as a consequence of deformation. Erosional denuda-

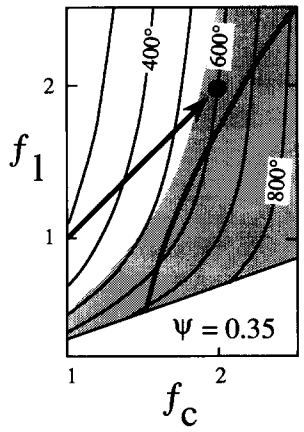

Fig. 11. Part of the $f_c - f_1$ plane showing the potential temperature at half crustal depth (i.e. $T_{c,p=1/2}$). For the parameter range adopted here (same as Fig. 4a) potential temperatures for homogeneously thickened lithosphere are $< 600\,^\circ C$ for $f < 2$. Quantitative time-dependent models for homogeneous lithospheric thickening with $f = 2$ and denudation on the timescale of 100 Ma show that actual temperatures attained are considerably less than the potential temperature, and may result in the generation and preservation of either glaucophane-schist or Barrovian assemblages depending on the thermal properties of the lithosphere [7,14]. The stippled region corresponds to deformation geometries which have the potential for lower crustal heating sufficient to generate significant volumes of melt, i.e., $T_{c,p=1} > 800\,^\circ C$ (see Fig. 4a). For these geometries the potential thermal structure may be significantly modified by magmatic advection of heat. The bold line represents the buoyancy force contour of 5×10^{12} Nm^{-1}.

tion sufficient to reduce all topography will result in exposure of mid crustal levels, where relatively limited total heating has resulted in the development of low to intermediate T and intermediate to high P metamorphics (i.e, glaucophane schist and Barrovian assemblages) depending on the limiting value of f_c (Fig. 11). Importantly, England and Thompson [14] and Sandiford [7] have shown that for part of the appropriate range of thermal properties (e.g. conductivity, heat production), homogeneous thickening of the continental lithosphere by a factor of ~ 2 may allow heating sufficient to stabilise the formation of glaucophane-schist assemblages.

For a given value of f_c the total heating for Type 3 paths will be much more significant than for Type 1 paths since not only is the potential temperature greater but also the thermal time constant significantly shorter. Indeed, Sandiford and Powell [13] show that, for geological plausible strain rates, greater than 50% of the potential heating may be achieved during the crustal thickening deformation. Since the temperatures achieved at shallow to intermediate crustal levels by conductive heat transfer along a Type 3 path are likely to be greatly augmented by heat advected by transport of melts generated at deeper crustal levels, peak temperatures may be coeval with the crustal thickening deformation, as appears to be the case in many high T–low P metamorphic belts [13,15]. Crustal thickening for Type 3 paths is necessarily limited by the limiting effective driving force for convergence, with limiting values of f_c much less than 2 for $f_{edc} <= 5 \times 10^{12}$ Nm^{-1} (Fig. 1). For small limiting f_c the amount of erosional denudation in order to reduce topography will also be small, eventually exposing relatively hot, low-intermediate pressure metamorphic terrains.

Orogens, or parts thereof, following Type 2 paths should show a close temporal relationship between heating and potential energy increases since both are effected by the decoupling of crust and mantle strains ($f_c > f_1$), with the increases in potential energy eventually terminating convergent deformation and, possibly, leading to the onset of extensional deformation. Indeed, the common occurrence of magmatism sourced within the lithosphere immediately following convergent deformation in ancient convergent orogens (so-called post-tectonic magmatism) testifies to such an interplay between their thermal and mechanical evolution and may be the hallmark of Type 2 paths [e.g. 2].

Acknowledgements

Without wishing to implicate them with any of the ideas expressed herein we thank Andy Barnicoat and Phil England for their reviews of an earlier version of this manuscript.

Appendix—Derivation of equations

The derivation of the equations for the change in elevation and potential energy follows closely the development of Turcotte [1] using the density distribution with depth, $\rho(z)$:

in the crust:

$$\rho(z) = \rho_c + \rho_c \alpha T_1 \left(1 - \frac{z}{f_1 z_1}\right) \quad \text{(A1)}$$

in the mantle lithosphere:

$$\rho(z) = \rho_1 + \rho_1 \alpha T_1 \left(1 - \frac{z}{f_1 z_1}\right) \quad \text{(A2)}$$

assuming the same thermal expansion for crust and mantle, and that the geotherm is linear (i.e. no heat production), with no conductive equilibration during deformation; these assumptions introduce negligible error as the α terms are second order.

Calculation of the isostatically-supported elevation change involves equating the vertical stress, σ_{zz}, at a common depth immediately beneath the lithosphere, for the undeformed and the deformed lithosphere respectively, where the vertical stress, σ_{zz}, is the integral of $\rho(z)$ with respect to z to the depth of interest:

$$g\int_{z_1'}^{h_0} \rho_0(z)\, dz - g\int_{z_1'}^{h_0+h} \rho_d(z)\, dz = 0 \quad \text{(A3)}$$

in which $\rho_0(z)$ is the density distribution in the undeformed crust, i.e. $\rho_0(z)$ is $\rho(z)$ at $f_1 = 1$ and $f_c = 1$; $\rho_d(z)$ is the density distribution in the deformed crust with specified f_1 and f_c; z_1' is the level to which density anomalies extend (i.e., the greater of z_1 and $f_1 z_1$); h_0 is the initial surface elevation of the crust; and h is the change of surface elevation. Equation (1), obtained by substituting (A1) and (A2) in (A3) and integrating, includes the simplification of substituting ρ_1 for ρ_c in the second term of (A1) introducing little error, again, because the α terms are second order [1].

The buoyancy force per unit orogen length, F_b, is given by the difference between the integrals of the vertical stress with respect to z, from the Earth's surface down to a common depth beneath the lithosphere, for the deformed and undeformed lithosphere respectively [1]:

$$F_b = \int_{z_1'}^{h_0} \sigma_{zz0}(z)\, dz - \int_{z_1'}^{h_0+h} \sigma_{zzd}(z)\, dz \quad \text{(A4)}$$

Parameters are as above, with, in addition, $\sigma_{zz0}(z)$, the vertical stress for $f_1 = 1$ and $f_c = 1$, and $\sigma_{zzd}(z)$, the vertical stress for specified f_1 and f_c.

The expression for potential temperature in terms of f_c and f_1 has been derived assuming a steady-state geotherm for a lithosphere with constant temperature top (0 °C) and bottom (T_1) boundary conditions, and with heat production constant with depth in the crust (ρH), and no heat production in the mantle [e.g. 16]. In terms of *initial* depths, T as a function of depth z in the crust, $T(z)$, is:

$$T(z) = \frac{T_1 - T_c}{f_1 z_1 - f_c z_c} f_c z + \frac{\rho H}{2k} f_c^2 z(2z_c - z) \quad \text{(A5)}$$

where T_c is the temperature at the base of the crust, and k is conductivity. Substituting $z = z_c$ in (A5), $T(z)$ is T_c, and the equation can be solved for T_c. Substituting $z = z_c$, $f_c = 1$ and $f_1 = 1$ into (A5) allows an expression to be derived for $\rho H/2k$ in terms of the initial T at z_c, T_c^0, as well as z_c, T_1, and ψ. Substituting these expressions for T_c and $\rho H/2k$ into (A5) gives the required equation, (3).

The proportional change in lithosphere thickness to re-establish the equilibrium heat flux through the base of the lithosphere assuming no conductive re-equilibration during heating, r_0, is obtained by comparing the initial heat flux with the flux after deformation. Thus:

$$\frac{T_1 - T_c^0}{z_1 - z_c} = \frac{T_1 - T_c^0}{r_0 f_1 z_1 - f_c z_c} \quad \text{(A6)}$$

Rearranging gives eqn. (4). To obtain r_p, an analogous expression is used except that T_c^0 on the right hand side is replaced with the potential temperature for $z = z_c$. The required potential temperature is different from eqn. (3) because the movement of the base of the lithosphere must be taken into account. This potential temperature is derived in the same way as above, but with $r_p f_1$ instead of f_1. Substituting this into (A6) and rearranging gives eqn. (5).

References

1 D.L. Turcotte, Mechanisms of crustal deformation, J. Geol. Soc. Lond. 140, 701–724, 1983.

2 G.A. Houseman, D.P. McKenzie and P. Molnar, Convective instability of a thickened boundary layer and its relevance for the thermal evolution of continental convergent belts, J. Geophys. Res. 86, 6115–6132, 1981.

3 P.C. England and G.A. Houseman, The mechanics of the Tibetan Plateau, Phil. Trans. R. Soc. Lond. A326, 301–320, 1988.

4 E.R. Oxburgh, Heterogeneous lithospheric stretching in the early history of orogenic belts, in: Mountain Building Processes, K. Hsü, ed., pp. 85–94, Academic Press, London, 1982.

5 N. White and D.P. McKenzie, Formation of the "Steer's head" geometry of sedimentary basins by differential stretching of the crust and mantle, Geology 16, 250–253, 1988.
6 M. Sandiford, Horizontal structures in deep crustal granulite terrains: a record of mountain building or mountain collapse? Geology 17, 449–452, 1989.
7 M. Sandiford, Secular trends in the evolution of metamorphic belts, Earth Planet. Sci. Lett. 95, 85–96, 1989.
8 P.C. England and D.P. McKenzie, A thin viscous sheet model for continental deformation, Geophys. J. R. Astron. Soc. 70, 295–321, 1982.
9 G.A. Houseman and P.C. England, Finite strain calculations of continental deformation, 1 Method and general results for convergent zones, J. Geophys. Res. 91, 3651–3663, 1986.
10 B. Parsons and D.P. McKenzie, Mantle convection and the thermal structure of the plates, J. Geophys. Res. 83, 4485–4496, 1978.
11 D.P. McKenzie, Some remarks on the development of sedimentary basins, Earth Planet. Sci. Lett. 40, 25–32, 1978.
12 C. Chopin, 1986 Coesite and pure pyrope from the western Alps: a first record and some consequences, Contrib. Mineral. Petrol. 86, 107–118, 1984.
13 M. Sandiford and R. Powell, Isostatic and thermal constraints on the evolution of high temperature low pressure metamorphic terrains in convergent orogens, J. Metamorph. Geol., in press, 1990.
14 P.C. England and A.B. Thompson, Pressure–temperature–time paths of regional metamorphism: 1. Heat transfer during the evolution of regions of thickened crust, J. Petrol. 25, 894–928, 1984.
15 R. Loosveld and M.A. Etheridge, A model for low-pressure facies metamorphism during crustal thickening, J. Metamorph. Geol., in press, 1990.
16 D.L. Turcotte and G. Schubert, Geodynamics: Applications of Continuum Physics to Geological Problems, Wiley, New York, N.Y., 1982.